J. Sustain. Metall. (2017) 3:168–178
DOI 10.1007/s40831-016-0093-1

THEMATIC SECTION: GREEN RARE EARTH ELEMENTS–INNOVATIONS IN ORE PROCESSING, HYDROMETALLURGY, AND ELECTROLYSIS

Influencing Factors on the Melting Characteristics of NdFeB-Based Production Wastes for the Recovery of Rare Earth Compounds

Stephanie Kruse[1] · Karoline Raulf[2] · Thomas Pretz[2] · Bernd Friedrich[1]

Published online: 3 November 2016

Abstract During the processing of neodymium-iron-boron (NdFeB) magnets, the blank is ground into its final form. During this step, there are slurries arising which contain major amounts of magnetic materials as well as lubricative and abrasive particles from the grinding disk. Since there is no tailor-made recycling process for this kind of wastes, a thermal treatment in combination with a melting step is proposed in this paper as a possible way for separating rare earth compounds from iron and other accompanying elements. During this process, a metallic Fe-based phase is separated from a rare-earth-containing oxide phase. Pretreatment has to be performed in order to separate the remainder of the cooling lubricant from the grinding process. Besides, the contents of accompanying elements such as oxygen have to be adjusted, since these elements can influence the melting process and phase separation. This paper deals with the factors which enable melting and phase separation by considering different input materials and the needed pretreatment. An oxygen content of more than 7 wt% needs to be maintained after the oxidation to enable phase separation during the melting. In addition, the presence of carbon is essential to avoid the formation of iron oxides. By this way, rare earth oxides from various NdFeB materials can be extracted with a high output and purity. This investigation shows that it is also possible to achieve an oxygen content of more than 7 wt% in different scraps produced by means of a thermal treatment. This provides an opportunity for making the recycling concept suitable for various kinds of scrap.

Keywords Grinding slurries · NdFeB magnet · Rare earth elements · Recycling

Introduction

Rare earth elements (REEs) and the supply of these elements from the western world have been discussed widely in the last few years. With their monopoly in the production of REEs, China had created a large supply deficit during the years 2009–2012 by limiting export quotas and increasing taxes for the export, after a huge overproduction in the preceding years leading to a corresponding price decline. Since this period, the avoidance of depending on Chinese production has been one big aim especially in Europe. However, there are only few primary resources in Europe which are exploitable, so other possibilities of securing supply of REEs have to be found. Till today, recycling of REEs from primary and secondary resources is not carried out on an industrial scale in Europe. One of the main reasons for the absence of recycling strategies is the lack of materials at disposal to be recycled since the export to China is less cost-intensive. Furthermore, with the sharp decline in the prices in recent years, the economic motivation to avoid the dependence on China also decreased, so there has been no industrially implemented recycling process. Due to the high content of rare earth elements, neodymium-iron-boron (NdFeB) magnets have a high secondary raw material potential; especially considering the production scraps that are used for this work. Notably,

The contributing editor for this article was Bart Blanpain.

✉ Stephanie Kruse
skruse@ime-aachen.de

[1] IME Process Metallurgy and Metal Recycling, RWTH Aachen University, Intzestraße 3, 52056 Aachen, Germany

[2] I.A.R Department of Processing and Recycling, RWTH Aachen University, Wüllnerstraße 2, 52056 Aachen, Germany

dysprosium, which is used as an alloying element in addition to neodymium, is considered to be particularly critical since it has low concentrations in most primary raw materials. Besides containing high concentration of REEs, production scraps offer the advantage of more precise knowledge of the components and for the avoidance of radioactive components, as they often occur in the primary extraction route. As stated in [1], grinding slurries with an oxygen content of more than 7 wt% can be molten with a phase separation taking place automatically. This could not be observed with slurries having a lower oxygen content. In combination with the presence of carbon, this is the main factor to enable the separation of iron and rare earth oxides. The present paper aims at proving that production scraps which are not already enriched in oxygen and carbon can also be processed in a similar way if a preliminary heat treatment is implemented.

Background

Characteristics of NdFeB Material

In general, NdFeB magnets consist essentially of the elements neodymium, iron, and boron, which form the hard magnetic alloy $Nd_2Fe_{14}B$. Stoichiometrically, this results in a distribution of approximately 26 wt% neodymium and 73 wt% iron. The boron content in most magnetic alloys is at a constant value of around 1 wt%. The fraction of REE varies depending on the particular application. This also applies to the other alloying elements such as cobalt, aluminum, copper, and gallium, which can be found in established magnets and which reduce the proportion of the main elements in some cases. Regarding REE, especially dysprosium has to be mentioned. Its presence increases the temperature stability of the magnet by shifting the Curie point to 450 °C through increasing the crystallization temperature of the hard magnet [2, 3]. Without the addition of dysprosium, the temperature ranges from around 80 to 100 °C. Dysprosium serves as a substitution element for neodymium, while its content in magnetic alloys can be up to 11 wt%. Besides dysprosium, praseodymium is a common substitution element for neodymium. The structure is obtained in a simplified form as shown in Fig. 1 [2, 4–6].

In addition to the main phase $Nd_2Fe_{14}B$ (Φ-phase) which represents around 85 wt% of the structure, especially a neodymium-rich phase as well as infrequent oxide particles are present. The neodymium-rich phase is located at the grain boundaries and covers around 12 wt% of the structure. Furthermore, another NdFeB phase can be found having the stoichiometry, $Nd_{1+\epsilon}Fe_4B_4$. The concentration of this phase with around 3 wt% is rather low. The compound is indicated as η-phase [2, 3].

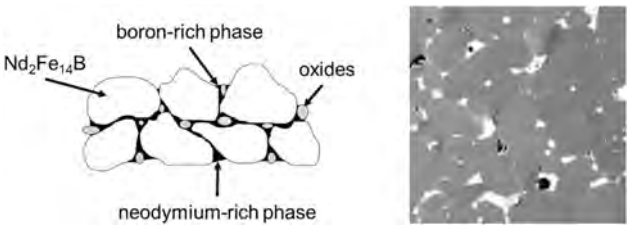

Fig. 1 Structure of NdFeB magnets according to [2]

Oxidation Potential of REEs

In order to investigate the oxidation potential of REEs, the Gibbs free energy of formation of REE oxides is used as evaluation criterion. The Richardson–Ellingham diagram is presented in Fig. 2 for selected elements and their oxides.

Figure 2 shows the Richardson–Ellingham diagram for selected metals and their oxidation reactions for pure substances, so that the activity of each amount is one. The lines are decoupled and have to be examined individually. Most real systems do not exist in the form of pure substances, but as mixture. The lines in the Ellingham diagram are then repositioned by the now lower activity of the respective substances. From the Richardson–Ellingham diagram results therefore, it can be observed that REEs have the highest oxygen affinity. However, this refers to the observation of pure substances. Taking into account the alloys, a determination of the respective activity is necessary, which cannot be carried out due to lack of thermodynamic data in this case. The difference between the Gibbs free energies of oxide formation of REEs and Fe is wide enough that oxidation of REEs still is preferred to that of Fe, but the lines might run closer to each other than that presented in Fig. 2.

Oxidation and Melting of NdFeB Material

The melting of magnetic material with the addition of Fe_2O_3 as oxidation agent leads to the structure shown in Fig. 4. Melting was carried out using a vacuum induction furnace with fragmented production scrap of NdFeB magnets. 100 g of material was mixed with the stoichiometric amount of Fe_2O_3 needed for the oxidation of the contained REEs. Subsequently the mixture was heated to a temperature of 1700 °C and kept at this temperature for 10 min. The structural analysis of the sample after cooling has been carried out by SEM/EDX. By considering the gray shade in the BSE picture, Fig. 3a, conclusion on the molar mass of the element can be drawn. The lighter a particle is represented, the heavier it is. Particularly, bright particles are therefore rich in neodymium and other REEs, while a darker color indicates the presence of iron. The average shade of gray, in this case represents the remaining

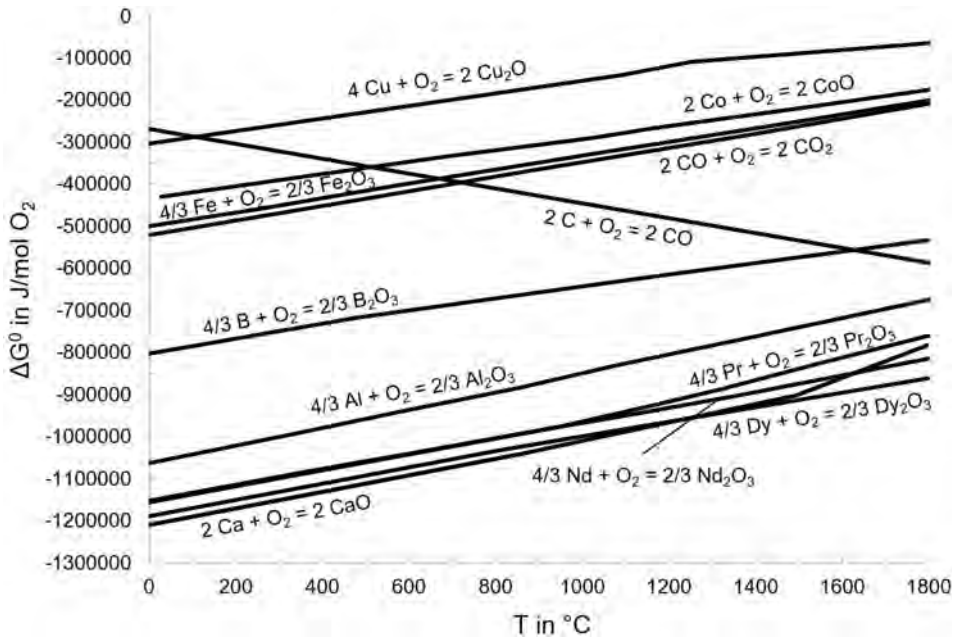

Fig. 2 Richardson–Ellingham diagram for selected elements and their oxides based on pure substances calculated using FactSage™

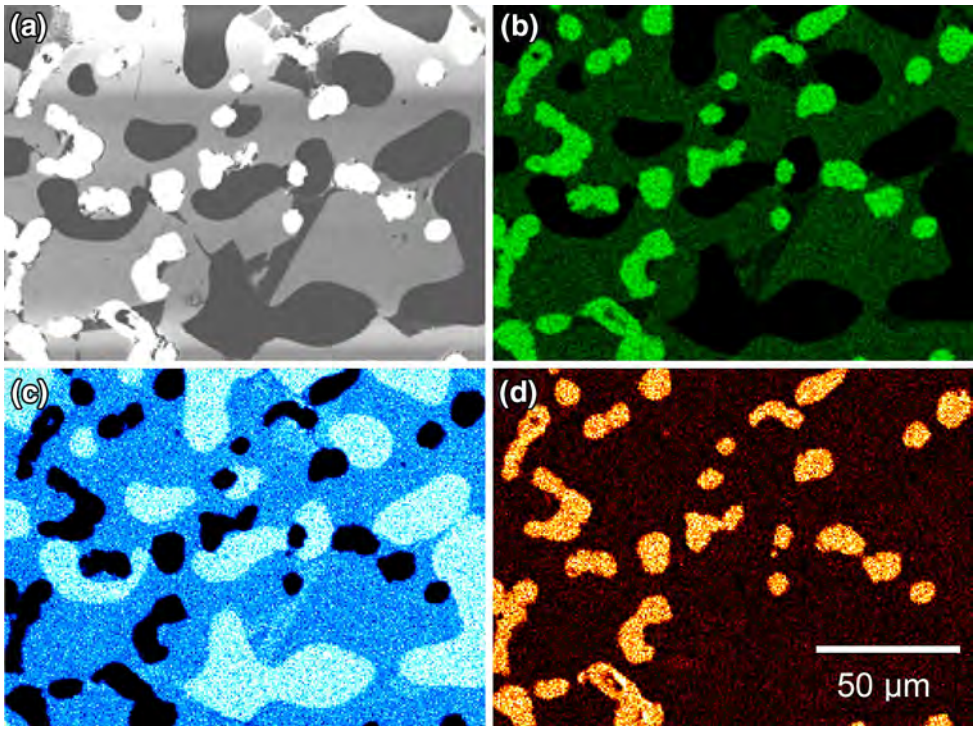

Fig. 3 SEM mapping of molten magnetic material: **a** BSE picture, **b** Nd, **c** Fe, **d** O

Φ-phase. The remaining pictures show the concentrations of Nd, Fe, and O (Fig. 3b–d), respectively.

In Fig. 3, a clear separation of neodymium and iron in the smaller particles can be seen. The background shows that both elements are still present, so an NdFe compound is present. Because neodymium is represented as significantly weaker, it can be concluded that a reformation of $Nd_2Fe_{14}B$ has taken place within solidification. However, the smaller particles show a pure iron phase, and the formation of neodymium. The oxygen concentration is constantly increasing in the particles in which Nd is present, while in the iron phase, no increase in contents is observed. This is also confirmed at the microscopic level. The oxygen affinity of REE is much higher than that of iron, resulting in a complete reduction of the iron oxide, according to the REM images. Edgley et al. [7] have investigated the

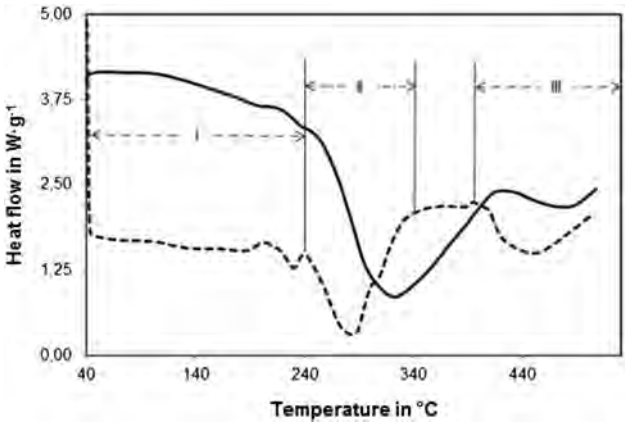

Fig. 4 DSC curve of the powdered magnet under oxygen (*dotted line* indicates the first derivation) [7]

prevailing mechanisms in the high-temperature decomposition of the magnetic material. To characterize the reactions, experiments were performed in air and oxygen and evaluated calorimetrically. For this purpose, magnets have been used in powder form, precise composition of which is not specified.

The calorimetric measurements have been carried out by Edgley et al. [7] using a differential scanning calorimetry (DSC) under pure oxygen atmosphere. As can be seen in Fig. 4, the obtained curve can be divided into three parts.

For zone I, which lasts from the beginning of the measurement up to 240 °C, the oxidation of the neodymium-rich phase at the grain boundaries is likely. Zone II (240–400 °C) represents the actual decomposition of the $Nd_2Fe_{14}B$ phase to metallic iron and Nd_2O_3, and the formation of pure boron. Zone III, which begins at 400 °C, then represents the oxidation of iron to Fe_2O_3, which is attributable to the high oxygen supply of the experiment conducted. The reactions are shown in the following Eqs. 1–3:

$$2NdO + \frac{1}{2}O_2 = Nd_2O_3 \quad (1)$$

$$Nd_2Fe_{14}B + \frac{3}{2}O_2 = Nd_2O_3 + 14Fe + B \quad (2)$$

$$2Fe + \frac{3}{2}O_2 = Fe_2O_3 \quad (3)$$

This is in contrast to earlier studies, which have assigned the three zones of the oxidation of the main components of the magnetic alloy. Oxidation of the η-phase, however, cannot be observed at any time. This finding is supported by XRD images of samples that have been heated up in the respective zones. Thus, the Φ-phase can be detected mainly before the treatment, but for the η-phase and for NdO_x, corresponding peaks also are detectable. The latter corresponds to the neodymium-rich phase. In other samples, corresponding to the heating treatment in zone I, cubic Nd_2O_3 also can be detected, while NdO_x is only weakly represented. In addition, peaks appeared, which can be associated with the formation of α-Fe. The intensity of the peaks of the Φ-phase diminishes during the heat treatment in zone II, when α-Fe appears more clearly and h-Nd_2O_3 is formed. At this time, the neodymium-rich phase cannot be detected. For samples which have been heat treated in zone III, this non-detectability also applies to $Nd_2Fe_{14}B$. This can no longer be detected beyond 400 °C. Although the α-iron peak is still visible, it is weakened by the formation of Fe_2O_3.

In summary, it can be stated that as the significant reaction, the decomposition of $Nd_2Fe_{14}B$ to Fe and Nd_2O_3 is proposed. That the formation of $NdFeO_3$ only takes place is based on the reaction of Nd_2O_3, and the later-formed Fe_2O_3 becomes nearly irrelevant.

State-of-the-Art and Own Recycling Concept

Regarding the assessment of the recycling situation, it is necessary to distinguish between the pre-consumer wastes and post-consumer wastes. The main difference is in the purity and access possibilities. While different types of production scraps typically arise in single-variety and are not mixed with other scraps, provided they are not supplied to value material recycling, retrace waste streams are much more complex to use. This occurs especially in case of magnets, since they are usually only a small part of a component and cannot be separated from this without major effort. Most of the approaches that can be found in literature thus relate to single-variety production scraps. Access to post-consumer scraps is hardly addressed [8].

The flow diagram shown Fig. 5 is described by Tanaka et al. [8] as state-of-the-art technology for processing broken production scrap and NdFeB grinding slurry that accumulate during production.

According to the illustrated process route, magnetic scraps are only exempted from the previously applied coating by wet or mechanical treatment, since the coating would impose impurities in the subsequent process steps, which could subsequently become included in the production route again. The grinding slurry is subjected to high-temperature oxidation which transfers the metallic components into the oxide phase. This is done especially in terms of safety, since due to the high oxidation potential of the REEs, grinding slurry has a significantly pyrophoric nature and a tendency to ignite spontaneously under the influence of atmospheric oxygen. After oxidation, the residue contains RE oxides as well as mainly iron oxide and the remaining components in oxidized form. This oxide intermediate is completely fed to the leaching process. After dissolution, precipitations of iron, boron, and

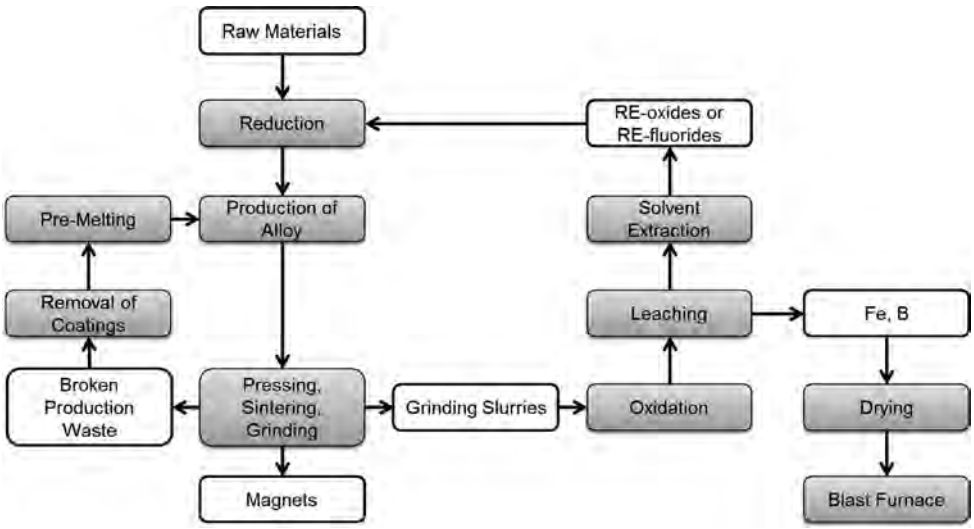

Fig. 5 State-of-the-art technology for the treatment of grinding slurries based on [8]

other minor elements take place, while the REEs stay in solution. The solution is fed to solvent extraction in which the separation of REEs is done to allow for subsequent feeding into a primary winning reduction process.

The recycling concept which is the basis for the investigations in this paper is described in detail in [1]. It is based on the treatment of grinding slurries, which have been stored and therefore show a higher oxygen content than other scraps. As seen in Fig. 6, a solid–liquid separation needs to be carried out to minimize the content of lubricant.

Afterward, the grinding slurry is stored under water to ensure the oxygen content remains high enough. In order to remove the organic components from the material, a pyrolysis needs to be carried out at a temperature of 600 °C. This also consolidates the remaining carbon. Afterward, the separation melt takes place in which the REEs are enriched as oxides in the slag phase, while iron remains in its metallic form. The produced RE oxide (REO) is suitable to be processed in the common REE route via a hydrometallurgical treatment and subsequently Nd or a REE alloy is produced in a molten salt electrolysis. In contrast to other investigations, for example, carried out by Yang et al. [9] who combined a thermal slag treatment with the hydrometallurgical processing, the present paper focuses on non-use of any additives in the slag during melting in order to avoid the lowering of the concentration of REO.

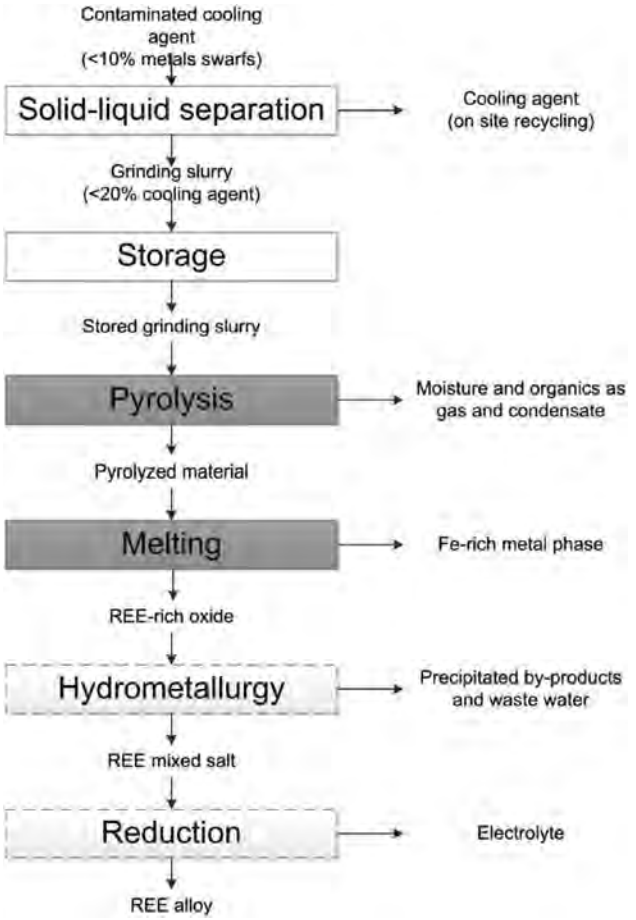

Fig. 6 Process flow sheet of the own recycling concept for grinding slurries [1]

Previous Experimental Work

For melting of NdFeB material a vacuum induction furnace is used. Inside the coil a graphite crucible is placed in which the material is inserted. The furnace is evacuated two times and finally filled with argon up to a pressure of 750 mbar. The material is heated up to the melting point, which is indicated by a considerable shrinking of the material due to sintering processes. However since there is a huge variation in melting temperature an exact value

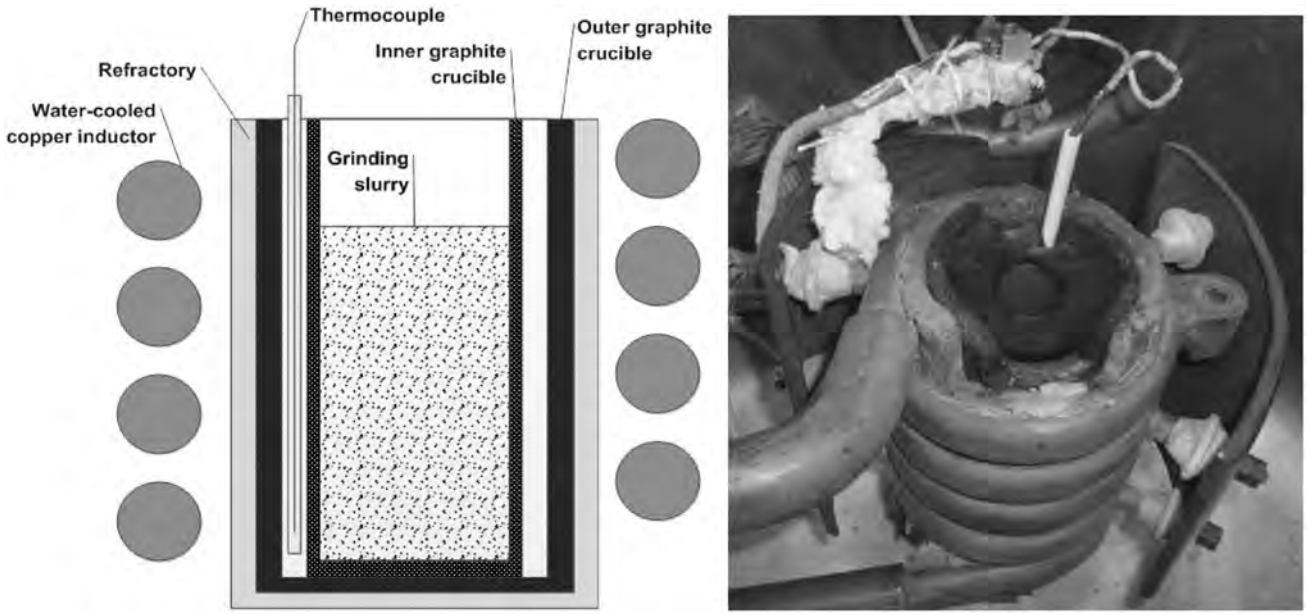

Fig. 7 Schematic setup of the melting trials (*left*) and coil with inserted crucible and material (*right*) [1]

cannot be given. The melting procedure is shown in Fig. 7 and described in detail in [1].

The output of the melting process should comprise two phases which are clearly separated from each other: one consisting mainly of RE oxides, and the other one being a cast iron.

The phase separation after solidification is shown in Fig. 8. The evaluated smelting experiments show a successful separation of iron and rare earth elements by performing a separation melt. Decisive requirement for this is a sufficiently high oxygen concentration in the feedstock. The phase separation can be performed reproducibly for O contents of 7 wt% and above.

The oxidation of iron can be avoided even at high levels of oxygen, providing that an inert gas is selected for the melting process. This is substantiated by the presence of carbon. It is added with the coolant and remains as consolidated coke in the material after pyrolysis. A second option to introduce carbon is the use of a carbon crucible. This can indeed make quantification difficult, since a discharge in the form of CO/CO_2 via the gas phase takes place, but it can be assumed that only that much amount of carbon is released until all excess oxygen has been discharged and a saturation of the metallic phase is reached. Analysis shows that carbon barely can be found in the oxide phase, which confirms the absence of carbon solubility. The detected levels are therefore likely due to inclusions in the slag phase, which may be due to erosion of the crucible.

As shown in the analysis, more than 95 % of REEs may be extracted in the form of oxides of the metallic phase,

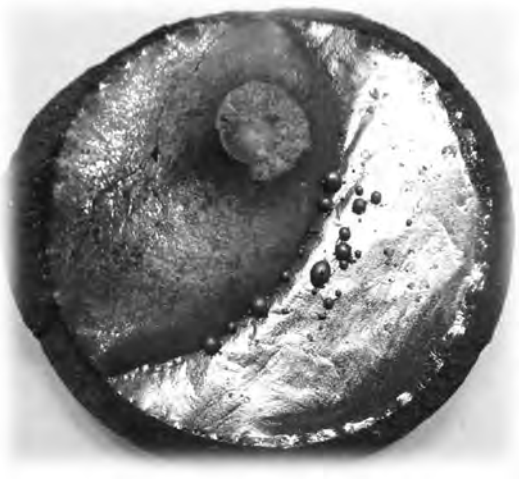

Fig. 8 Phase separation after melting of grinding slurries: metallic iron phase (*right*), REE-rich oxide phase (*left*)

with the purity level being over 90 %. Purity is in particular reduced by the formation of boron oxide and aluminum oxide. However, both lead to a reduced density, which among other things such as interfacial tension and viscosity, enables the phase separation.

The theoretical analysis of the densities of the phases generated suggests that there should be no phase separation, since these are kept at a similar magnitude. The density of iron is 7.85 g/cm^3 while the density of Nd_2O_3 is 7.2 g/cm^3. According to the elemental analysis, the presence of cast iron is likely which reduces the density to 7.2 g/cm^3, whereby there is only a small deviation to

Table 1 Measured densities of different samples of metallic and oxide phases via pycnometer

	Density of oxide phase	Density of metallic phase
Sample 1	5.81	7.04
Sample 2	5.79	6.84
Sample 3	5.74	9.19

Nd_2O_3. The formation of cementite (Fe_3C) is conceivable; however, it can be largely ruled out due to the high melting point of over 1800 °C.

In order to verify the differences in density, density analysis have been carried out using a gas pycnometer. Here, the density of a substance is calculated out of its mass and its volume. Table 1 shows the densities of the metallic and oxide phases of three different samples.

It can clearly be seen that the densities throughout differ by at least 1 g/cm^3 so that the phase separation can be realized in this way readily. In this case, a high interfacial tension between the boundary surfaces of metal/oxide and oxide/graphite crucible plays supportive role. These interfacial tensions cannot be measured because of the elevated temperatures but can be seen in the separated phases as shown in Fig. 9.

Materials and Methods

Material Characterization

In Table 2 the compositions of two grinding slurries (M1 and M2) are compared with an untreated grounded magnet M3. The analysis has been carried out using ICP-OES for the metals and carrier gas hot extraction for oxygen, carbon, and nitrogen.

As can be seen in the table, the REE contents show obvious variations which indicate the wide ranges in which especially the alloying elements can be found in magnetic material. However, the sum of all REEs is nearly the same. The most obvious difference between grinding slurries and the magnetic materials can be found in the contents of oxygen and carbon, written in bold characters. Due to the storage of the grinding slurry under water for safety reasons, a large oxygen uptake has taken place. Carbon is introduced during the grinding process as component of the lubricant and the grinding media.

Setup and Trials of the Thermal Treatment

For the oxidation trials, material M3 is used since no prior oxidation has taken place. Thus, it can be guaranteed that any kind of oxygen enrichment that is noticed is due to the thermal conditioning of the magnetic material. The experiments are performed in a vacuum induction furnace with a known vessel volume, so that a defined quantity of a gas mixture of argon and oxygen may be supplied. AS the water-cooled vessel is used, the furnace is called cold-wall furnace. The water-cooled coil is traversed by an alternating current, whereby an alternating magnetic field is built up. This results in an induced voltage in the susceptor which causes eddy currents whereby heat is generated. Either metallic or graphite container can serve as susceptor. The setup is shown in Fig. 9.

The furnace has a maximum power of up to 4 kW, which heavily depends on the crucible (material, wall thickness, etc.) and the feedstock. The water-cooled vessel

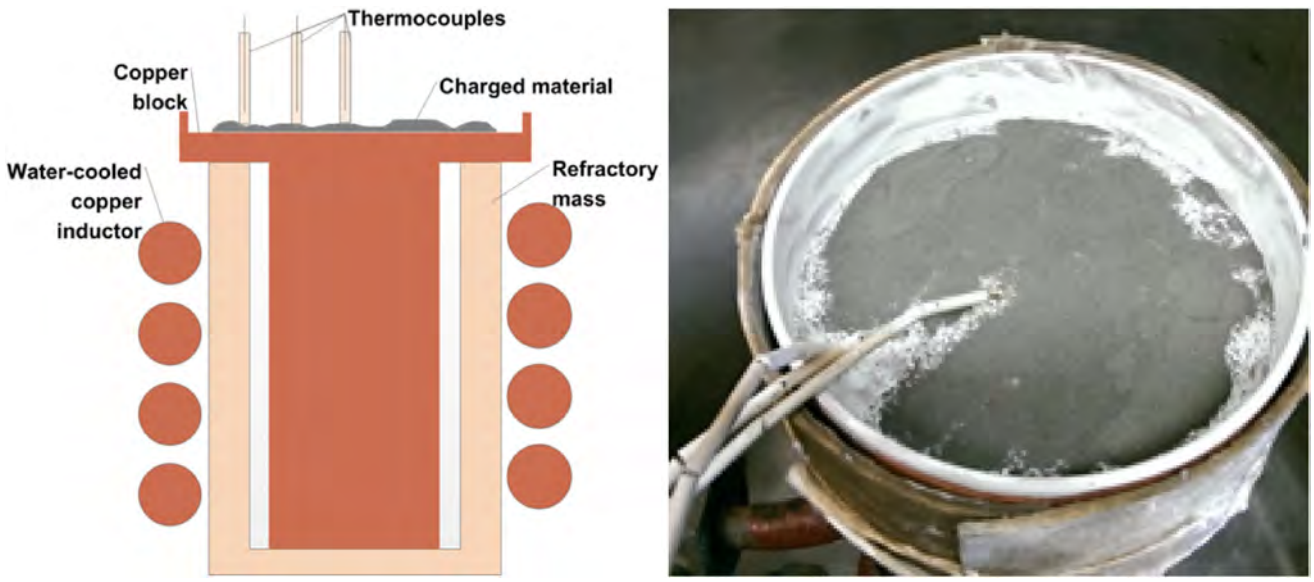

Fig. 9 Setup of the thermal treatment for grounded magnets, schematic (*left*) and top view (*right*)

Table 2 Compositions of two grinding slurries and a grounded magnet

Element	Content (wt%)		
	M1	M2	M3
Nd	15.90	18.10	20.65
Pr	4.66	0.10	3.98
Dy	6.11	8.58	2.04
Co	0.98	2.84	0.82
Cu	0.23	0.11	0.13
B	1.05	0.89	1.03
Al	0.57	0.17	0.27
O	**4.48**	**7.98**	**0.5**
C	**1.56**	**0.41**	**0.1**
N	0.0640	0.0649	n.s.
Fe	62.66	60.49	Matrix

Table 3 Parameters of the thermal-treatment trials

Trial number	Temperature (°C)	Ratio Ar/O_2 (%)	Pressure (mbar)	Dwell (min)
1	550	99/1	800	15
2	550	99/1	800	15
3	550	99/1	300	15
4	550	99/1	300	15
5	550	99/1	450	15
6	300	99/1	450	15
7	550	99/1	800	15
8	600	99/1	600	15
9	300	99/1	600	60
10	550	99/1	800	90
11	550	96/4	800	15
12	600	96/4	600	15
13	550	96/4	600	60
14	600	79/21 (N/O_2)	1000	60

has a volume of 80 L. The heating is done by inducing eddy currents into the plate on which the feedstock material is located on. To avoid oxidation of the copper plate, it is coated with boron nitride. The experimental design for the tests is shown in Table 3.

The aim is to verify under which conditions the currently accepted limit of 7 wt% oxygen can be achieved as precisely as possible. After adjusting the process pressure, the heating to the target temperature is done by controlling the power, wherein the heating has to take place as uniformly as possible during the specified time interval. Due to manual control, this can only be ensured partly. Upon reaching the target temperature, it is maintained there for a particular dwell period. Due to the inductive heating and its manual control, temperature fluctuations of 10 °C have been recorded. After dwelling, the power is switched off, and the furnace evacuated again to prevent further oxidation during cooling time. Due to the isolation of the copper plate, the cooling time is set to 5 h, so that further temperature-induced phase transformations and progressive reactions with oxygen present cannot be ruled out.

Fig. 10 Oxidized material after the trial

After cooling the samples, especially after experiments with a high temperature and high oxygen content, the sintered material showed a light blue-colored surface. This is shown in Fig. 10. A sample of the material is extracted and fed to oxygen analysis via carrier gas hot extraction without crushing.

Analytics and Discussion

This section focuses on the results of the thermal treatment of magnetic material as well as on analyzing differences in grinding slurries which can be melted and those which cannot be processed. The results of the oxygen analysis are considered according to these findings, and a set of related reactions is proposed.

Grinding Slurries

The grinding slurries M1 and M2 are analyzed via XRD after pyrolysis and compared to an untreated grinding slurry to get information about the phases which occur after pyrolysis.

According to X-ray diffraction analysis, the starting material consists entirely of the magnetic alloy $Nd_2Fe_{14}B$. Other phases cannot be detected in significant amounts. By pyrolysis, the majority of $Nd_2Fe_{14}B$ is decomposed to form α-Fe, RE-carbides, oxides, and RE-$NdFeO_3$. Here considerable differences in the structural compositions of the pyrolysis products are observed. The decomposition of

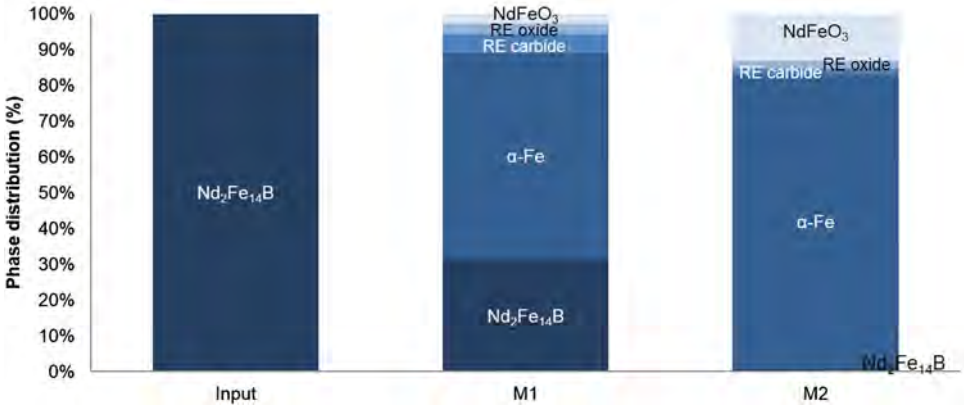

Fig. 11 Phase distributions of different pyrolyzed grinding slurries compared with untreated materials

$Nd_2Fe_{14}B$ is less pronounced in M1, so that a residual content of >30 % is still detectable. The proportion of the produced α-Fe is correspondingly low, whereas in M2, it is over 80 %. Another striking point is the relatively high proportion of $NdFeO_3$ in M2. While the content of RE oxides is similar, which is probably due to the oxidation of the Nd-rich phase at M1, a stronger formation of carbides can be listed. Thus, the explanation for a successful melting is apparently to be found in the incomplete decomposition of the magnetic phase and the formation of RE-carbides or missing $NdFeO_3$. Due to the absence of oxygen, the carbon reacts with the present REEs to form carbides. Because of its small proportion, boron cannot be detected or quantified in the composition of the phases formed, so that no statement can be made about the whereabouts of boron. In Fig. 11, a representation of the values in the form of bar charts is given, which clarifies the decomposition processes [1].

Figure 12 shows an oxygen mapping for the material M2. Bright areas are rich in oxygen, while dark areas have a rather low oxygen content.

The mapping in Fig. 12 clearly shows that the particles formed surface layers which are very rich in oxygen compared with the rest of the particle. These outer layers cannot be detected in the recordings of material M1. For this reason, it can be assumed that by the thermal treatment of oxidized material, a kind of corrosion of $Nd_2Fe_{14}B$ particles leads to the formation of an oxygen-rich surface layer. This decomposition of the original alloy composition affects apparently significantly the melting behavior of the material. Possibly caused by a eutectic system, the compound has a lower melting point. The formation of the boundary layer under a disintegration of $Nd_2Fe_{14}B$ shows good accordance with the results of XRD recordings. According to this recording, the $Nd_2Fe_{14}B$ phase only exists to a minor degree in M2.

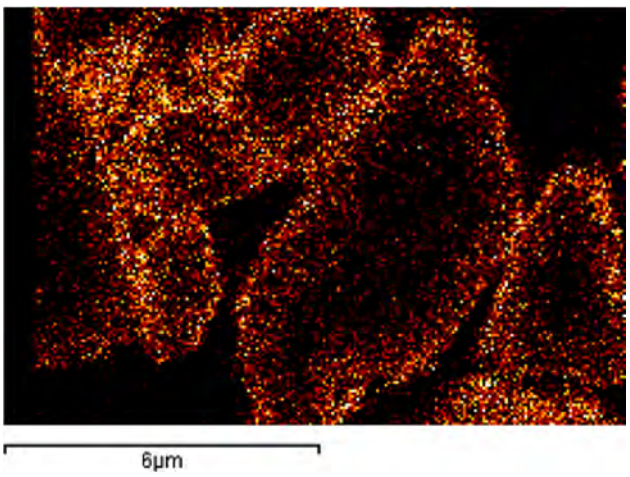

Fig. 12 Oxygen mapping of material M2

Magnetic Material

The experiments shown in Table 3 are sampled and subjected to oxygen analysis. The oxygen contents obtained are shown in Table 4. The analysis has been performed by

Table 4 Oxygen contents of the samples treated according to Table 3

Trial number	O_2 (wt%)	Temperature (°C)	Pressure (mbar)
1	5.95	550	800
2	5.79	550	800
3	1.95	550	300
4	2.65	550	300
5	2.40	550	450
6	1.45	300	450
7	5.33	550	800
8	5.48	600	600
9	1.45	300	600
10	8.70	550	800
11	6.45	550	800
12	5.42	600	600
13	6.16	550	600
14	23.18	600	1013

carrier gas hot extraction. In each case, the values are averaged of a double determination to compensate the inhomogeneity of the material. Due to the high reactivity of the material and because of changing input compositions, the inhomogeneity cannot be eliminated.

Significant finding is that an uptake of oxygen of about 7 wt% is possible. This has been defined as the lower limit for allowing the melt. However, this requires high temperatures, and a significantly over-stoichiometric oxygen supply is necessary. To determine the influence of the oxygen concentration, the content in the gas was increased. As can be seen in trials 11–13, a significantly increased oxygen content cannot be detected. A crucial factor is also the process temperature. This has, according to the analysis, no linear influence on the absorption of oxygen; however, experiments 6-9 suggest that the absorption of oxygen is made possible only from a certain temperature. To this end, an activation energy is necessary to start the oxidation. Until this critical temperature is exceeded, the oxygen uptake depends on the pressure in the furnace and the holding time. The holding time in this case has the greatest influence on the oxidation of the material, making it the most effective leverage with respect to the adjustment of the oxygen content. A certain temperature is required for initiating this process.

For the SEM/EDX analysis, the fully oxidized material from trial 14 is used to demonstrate the effects occurring with certainty, as in this experiment, the highest oxygen content has been recorded in the material. XRD analysis for these trials showed no evidence of any RE phase being present which is why these analyses are not considered in this paper.

The focus was especially on the determination of the surface layers, which have been already detected in heat-treated material beforehand. The micrograph of trial 14 is shown in Fig. 13. The formation of a boundary layer around the particles can be clearly seen.

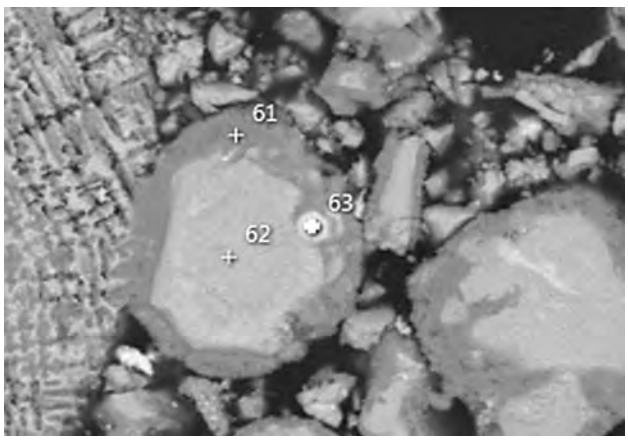

Fig. 13 SEM picture of oxidized magnetic material (trial 14)

Table 5 Composition of the measurement points from Fig. 13

	O (wt%)	Fe (wt%)	Pr (wt%)	Nd (wt%)	Dy (wt%)
Point 61	35.2	61.5	0.6	2.1	0.6
Point 62	30.0	28.8	6.9	24.3	10.0
Point 63	25.4	5.6	12.2	40.6	16.2

The analysis of the polished sample is shown in Table 5. The analysis suggests that the apparent surface layer is iron oxide, which contains only small amounts of REEs, while the core probably consists of the mixed oxide RE-FeO3. The much brighter particle (measurement point 63) again shows an enrichment of RE oxide, which in return is characterized by a low Fe content.

The analysis presented here can be vague due to the significantly fluctuating results which may obscure any final assessment; it can be stated, however, that the provision of oxygen always results in a decomposition of the Φ-phase.

Based on the previously mentioned findings, the following reactions (Eqs. 4–7) can be proposed. The reactions are mainly based on those of [7], but in addition consider the presence of the mixed oxide $NdFeO_3$.

$$2NdO_x + \frac{(3-2x)}{2}O_2 = Nd_2O_3 \quad (4)$$

$$NdO_x + \frac{(4+x)}{2}C = NdC_2 + x/2CO_2 \quad (5)$$

$$Nd_2Fe_{14}B + \frac{3}{2}O_2 = 2NdFeO_3 + 12Fe + B \quad (6)$$

$$2Fe + \frac{3}{2}O_2 = Fe_2O_3 \quad (7)$$

The first two reactions show that a certain amount of rare earth oxides and rare earth carbides is produced. The decomposition of $Nd_2Fe_{14}B$ proceeds by forming a mixed oxide and iron which is oxidized if sufficient oxygen is present.

Conclusion and Outlook

The oxidation experiments presented in this paper follow the objectives set out above; however, a thermal pre-treatment is also required when using grinding slurries from the point of separation of the coolant. This affects the process management of the following melting processes by the evaporation of the lubricative components. This aspect has not been considered in the experiments as they were carried out to limit the consideration purely on the oxidizability of the magnetic material. The separation of the coolant from grinding slurry and the processes occurring in

the pyrolysis mechanisms are set out in more detail in [10]. The key finding is that in separating the lubricant, a temperature of about 600 °C must be achieved in order to effectively separate the hydrocarbons contained and reduce the reactivity of the carbon remaining [10].

The oxidation experiments show that adjusting the oxygen content is possible by a temperature treatment. However, this requires an activation energy in the form of exceeding a critical temperature. This is in accordance with the experiments carried out at about 300 °C. By exceeding the temperature, an oxygen uptake of more than 2–3 wt% can be realized. The main parameters are the furnace pressure and the holding time or duration of the experiment. At a pressure of 800 mbar and a test period of 90 min, an oxygen content of above 8 wt% can be achieved. Here, however, a very large surface area of the magnetic particles is required to ensure the contact of the material to the furnace atmosphere.

A pre-treatment step for the pyrometallurgical processing should therefore comply with the requirements of a high-temperature oxidation as well as the removal of the disturbing melt impurities. In this context, the choice of a furnace is conceivable which ensures the contact of all particles with the atmosphere, which can be operated gas-tight, but also has a corresponding extraction and subsequent gas treatment equipment, such as a rotary kiln.

The aim of the melting trials, and thus the production of a RE-rich oxide with the separation of iron, can be achieved reproducibly using knowledge of the main influencing factors. The process temperature depends widely on the input material and therefore cannot be determined exactly. The upper temperature limit has been set at 1550 °C. The conditions for a successful separation melt are an oxygen content of 7 wt% or higher as well as a carbon content of around 2 wt%. With the introduction of oxygen a decomposition of the hard magnetic Φ-phase takes place with the formation of $NdFeO_3$ and α-iron. These phases enable the melting at lower temperatures. Carbon supports the low process temperature via formation of a cast iron and reacts with excessive oxygen in form of CO/CO_2. In the experiments more than 95 % of the REE can be extracted from the metal. Due to the additional extraction of aluminum and boron in form of their oxides, the purity of REO is above 90 wt%. However, a further increase does not appear desirable, because the contents of B_2O_3 and Al_2O_3 lower the density of the oxide phase to such an extent that the phase separation is made possible between the metallic and oxide phase. A scaling up of the tests is necessary to evaluate the extraction and the final purity.

In summary, it can be said that the recovery of REEs with high yields and purities from NdFeB magnets with the processes presented in this paper is possible. The hydrometallurgical treatment is necessary to separate the oxides of boron and aluminum. The possibility of directly reducing different rare earth oxides at the same time has not been ascertained in this work, but there is an opportunity to reduce the amount of chemicals needed in the proposed processes. The biggest challenge to be faced is the high energy consumption of a two-stage heating as wells as the batch-wise operation which would be done.

The experiments carried out suggest that the separation melt allows for a very robust process and a high flexibility with respect to the starting materials. The thermal treatment allows for the adjustment of the oxygen content and can thus compensate for variations in the input streams. Carbon, unless present in the feedstock, can be added by choosing graphite as crucible material. Accordingly, the transferability of the process to other production scraps as well as on post-consumer scrap is conceivable, resulting in a significantly higher amount of feedstock. However, for the industrial-scale implementation, the economic, ecological, and political impetuses are currently missing.

References

1. Kruse S, Raulf K, Trentmann A et al (2015) Processing of grinding slurries arising from NdFeB magnet production. Chem Ing Tech 87(11):1589–1598. doi:10.1002/cite.201500070
2. Rodewald W, Katter M, Reppel GW (2002) Fortschritte bei pulvermetallurgisch hergestellten Nd-Fe-B Magneten (Progress in the powder metallurgical production of Nd-Fe-B magnets). Hagener Symposium Pulvermetallurgie 18:225–245
3. Grieb B, Henig E, Schneider G et al (1992) Phase diagrams of Fe Nd b and related systems for optimization of hard magnetic properties. Powder Metall 35(3):221–227
4. Li S, Bi H, Yuan Z et al (2005) Thermodynamics and heat treatment of B-enriched nanocomposite NdFeB alloys containing Dy. Appl Phys A 80(2):313–316. doi:10.1007/s00339-003-2148-y
5. Kablov EN, Petrakov AF, Piskorskii VP et al (2005) Effect of praseodymium on magnetic properties and phase composition of a material of the Nd–Pr–Dy–Fe–Co–B system. Met Sci Heat Treat 47(5–6):227–231
6. Hatch G (2011) Seagate, rare earths and the wrong end of the stick. http://www.techmetalsresearch.com/2011/07/seagate-rare-earths-and-the-wrong-end-of-the-stick/. Accessed 30 Nov 2015
7. Edgley DS, Le Breton JM, Steyaert S et al (1997) Characterisation of high temperature oxidation of Nd-Fe-B magnets. J Magn Magn Mater 173(1–2):29–42. doi:10.1016/S0304-8853(97)00189-3
8. Tanaka M, Oki T, Koyama K et al (2012) Recycling of rare earths from scrap. Handbook on the physics and chemistry of rare earths, vol 43. Elsevier, Amsterdam, pp 159–211
9. Abrahami ST, Xiao Y, Yang Y (2015) Rare-earth elements recovery from post-consumer hard-disc drives. Min Process Extr Metall. doi:10.1179/1743285514Y.0000000084
10. Raulf K (2015) Recycling von Schleifschlämmen aus der NdFeB-Magnetproduktion—Vorkonditionierung für die metallurgische Verwertung (Recycling of grinding slurries from NdFeB magnet production-preconditioning for metallurgical utilization). Dissertation, RWTH Aachen University, Aachen